Characterizing the Spectral Properties and Time Variation of the In-Vehicle Wireless Communication Channel

Steven Herbert, *Student Member, IEEE*, Ian Wassell, Tian-Hong Loh, *Member, IEEE*, and Jonathan Rigelsford, *Senior Member, IEEE*

***Abstract*—To deploy effective communication systems in vehicle cavities, it is critical to understand the time variation of the in-vehicle channel. Initially, rapid channel variation is addressed, which is characterized in the frequency domain as a Doppler spread. It is then shown that, for typical Doppler spreads, the in-vehicle channel is underspread, and therefore, the information capacity approaches the capacity achieved with perfect receiver channel state information in the infinite bandwidth limit. Measurements are performed for a number of channel variation scenarios (e.g., absorptive motion, reflective motion, one antenna moving, and both antennas moving) at a number of carrier frequencies and for a number of cavity loading scenarios. It is found that the Doppler spread increases with carrier frequency; however, the type of channel variation and loading appear to have little effect. Channel variation over a longer time period is also measured to characterize the slower channel variation. Channel variation is a function of the cavity occupant motion, which is difficult to model theoretically; therefore, an empirical model for the slow channel variation is proposed, which leads to an improved estimate of the channel state.**

***Index Terms*—Vehicle cavities, reverberation chambers, electromagnetic cavities, Doppler spread, time correlation, autoregressive model, information capacity, underspread channels.**

I. Introduction

WIRELESS devices are increasingly deployed in vehicles [1]. To our knowledge there is no existing characterization of the time variation of the in-vehicle wireless communication channel, and such a characterization would lead to improved performance of a deployed wireless system. Specifically, it would be possible to evaluate the information capacity of the channel, and to use the statistical properties of the time variation model to improve channel estimation/ prediction. Throughout this paper, the property that the electromagnetic wave propagation in vehicle cavities is similar to that in a reverberation chamber is used [2], [3].

Any linear wireless channel can be completely characterized by its time varying impulse response, $h(t,\tau)$, where t is absolute time, and τ is time lapse since the impulse [4]. To characterize the channel in this way, however, requires knowledge of the joint probability distribution of the channel over all t and τ, which in reality is not usually achievable. Instead it has been observed that many real world channels can be assumed to be wide-sense stationary uncorrelated scattering (WSSUS) channels, which simplifies the analysis of $h(t,\tau)$ [4]–[6]. The usual justification for invoking the WSSUS assumption, is detailed in [[5]-Section-6.6]. To justify the uncorrelated scattering (US) model, the instantaneous propagation is modeled as a continuum of uncorrelated point scatterers. This approach is consistent with our previous findings [2], and also work undertaken by Chen [7] in a reverberation chamber. Concerning the wide-sense stationary (WSS) model, it seems reasonable that the correlation of two measurements is only dependent on the time interval between them. Preliminary work, detailed in Appendix A, indicates that the WSSUS model is indeed appropriate for the reverberation chamber, and we therefore continue to make this assumption for the remainder of the paper.

We approach the time variation of the in-vehicle channel, by first classifying the variation as either, 'rapid variation', or 'slow variation'. We propose that rapid variation is best understood by characterization in the frequency domain. We characterize the power spectral density (PSD), $P_H(f,m;\nu)$, where f and m are frequencies, and ν is the Doppler shift. Note that in general f and m can be different, however in this paper they are always the same, and hence the notation $P_H(f,f;\nu)$ is used throughout. The purpose of characterizing the channel Doppler spread is to evaluate the channel information capacity. For the WSSUS channel if $\tau_0\nu_0 \leq 1/4$ (where τ_0 is the maximum delay spread, and ν_0 is the maximum Doppler shift), then the channel is underspread [[8]-Section-IIB]. In this case the additive white Gaussian noise (AWGN) capacity, with perfect channel state information (CSI) at the receiver [9] can be

Manuscript received January 9, 2014; revised March 27, 2014 and May 23, 2014; accepted May 25, 2014. Date of publication June 4, 2014; date of current version July 18, 2014. This work was supported in part by the Engineering and Physical Sciences Research Council of U.K. and in part by the National Physical Laboratory under an EPSRC-NPL Industrial CASE studentship program on the subject of intravehicular wireless sensor networks. The work of T.-H. Loh was supported in part by the 2009–2012 Physical Program and in part by the 2012–2015 Electromagnetic Metrology Program of the National Measurement Office, an Executive Agency of the U.K. Department for Business, Innovation and Skills, under Projects 113860 and EMT13020, respectively. The editor coordinating the review of this paper and approving it for publication was E. K. S. Au.

S. Herbert is with the Computer Laboratory, University of Cambridge, Cambridge CB3 0FD, U.K., and also with the National Physical Laboratory, Teddington TW11 0LW, U.K. (e-mail: sjh227@cam.ac.uk).

I. Wassell is with the Computer Laboratory, University of Cambridge, Cambridge CB3 0FD, U.K. (e-mail: ijw24@cam.ac.uk).

T.-H. Loh is with the National Physical Laboratory, Teddington TW11 0LW, U.K. (e-mail: tian.loh@npl.co.uk).

J. Rigelsford is with the Department of Electronic and Electrical Engineering, University of Sheffield, Sheffield S1 3JD, U.K. (e-mail: j.m.rigelsford@sheffield.ac.uk).

Color versions of one or more of the figures in this paper are available online at http://ieeexplore.ieee.org.

Digital Object Identifier 10.1109/TCOMM.2014.2328635

approached in the infinite bandwidth limit [10]. We characterize the rapid variation in Section III.

Slow channel variation manifests itself at very small Doppler shifts, and therefore does not significantly affect the channel capacity. However, such a characterization allows the channel to be estimated as it slowly varies, which could lead to improved communication performance, including potentially feeding back CSI from the receiver to the transmitter. We characterize the slow variation in Section IV. Finally, conclusions are given in Section V.

A. Contributions

The main contributions of this paper are:

- Doppler spread measurements in-vehicles. To our knowledge this is the first published measurement of this kind.
- A bound on the PSD, given simple assumptions which apply to the vehicle cavity environment.
- Tracking the time variation of the in-vehicle channel as a first-order (AR1) process.

II. Experimental Method

We undertook measurements in three environments. First, we use the reverberation chamber to verify an important assumption, specifically that the time variation can be considered to be a WSSUS process. Secondly, in a metal cavity which has been verified to have vehicle-like properties [3], [11], this metal cavity was placed in a fully anechoic chamber that allowed us to perform tightly controlled measurements, having a very low noise floor (i.e., the anechoic chamber is shielded from external radiation, so only thermal noise is present). Finally, measurements were performed in an actual vehicle, which enabled us to measure the ground truth.

A. Measurements in Reverberation Chamber

To verify that the time variation of the channel is WSSUS, we focus on one specific form of time variation in electromagnetic cavities, specifically that owing to a large reflective rotating paddle in a reverberation chamber. Using the same logic as Karlsson *et al.* [12], we find the stationary S-parameters for each of 1000 paddle steps (i.e., the paddle rotates a one-thousandth of a complete rotation, and this is known as a paddle step), and then assert that the autocorrelation function of the continuously rotating stirrer is the same as that of the stepped stirrer, assuming the stirrer rotates at a constant velocity. These results are presented in Appendix A. We also use the measurements to verify a number of important assumptions in Section III-B.

B. Measurements in Vehicle Like Cavity

The vehicle like cavity is shown in Fig. 1 with origin and axes defined. It has dimensions 1260 mm $\times$ 1050 mm $\times$ 1220 mm was used to measure the Doppler spread caused by various forms of motion. We performed two measurement campaigns.

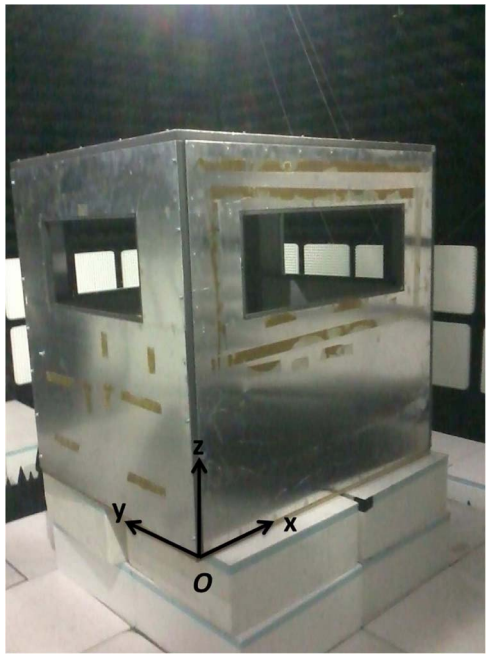

Fig. 1. Vehicle like cavity, with origin and axes defined.

In the first measurement campaign (the results of which are presented in Section III-A) a continuous wave sinusoidal signal was generated at 2.45 GHz (i.e., in the Industrial Scientific and Medical band used by *Wi-Fi*, *Zigbee* and *Bluetooth*), and connected via co-axial cable to a Schwarzbeck 9113 antenna, located at (850, 760, 660) mm, x-polarized (where x-polarized refers to the antenna orientation with direction of maximum E-field parallel to the x-axis). The PSD of the input signal is shown in Fig. 2 (which theoretically should be a perfect spike), and was the same for all the measurement campaigns. A Schwarzbeck 9113 antenna was also used as a receiver, located at (180, 760, 660) mm, also x-polarized, which was connected via a co-axial cable to an Agilent E4440A spectrum analyzer. For all the measurements, the antenna locations have been chosen arbitrarily. Four types of stirring were investigated:

1) A person leaning into the cavity and moving around, to mimic the situation where moving occupants disturb the electromagnetic wave propagation.
2) The rotating mechanical stirrer shown in Fig. 3(a), to mimic the scenario where a reflective object (i.e., a piece of luggage) is moving and thus disturbs the electromagnetic wave propagation.
3) A person leaning into the metal cavity and moving one antenna, to mimic a mobile to fixed channel in a vehicle (movement in the vicinity of its original location).
4) A person leaning into the metal cavity and moving both antennas, to mimic a mobile to mobile channel in a vehicle (movement in the vicinity of its original location).

In each case the presented measurement is an average over many single spectrum analyzer sweeps (either 25 or 50, though it made little difference). This allows the PSD to be more accurately estimated from the measurements.

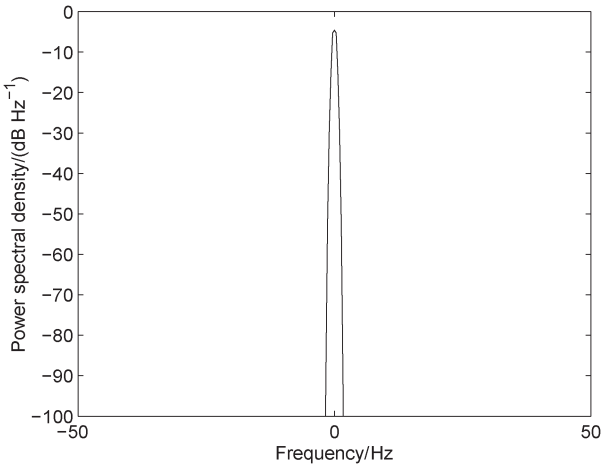

Fig. 2. Power spectral density of input signal.

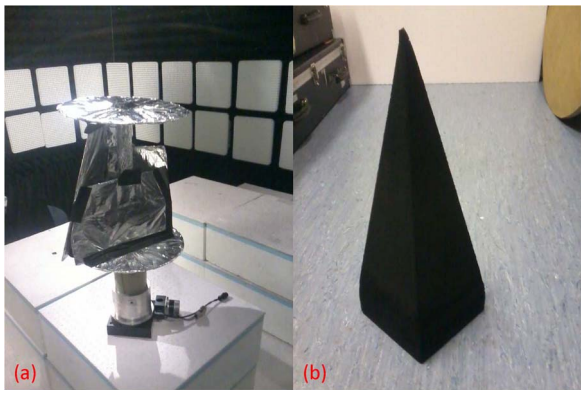

Fig. 3. (a) Mechanical stirrer; (b) a single unit of RAM.

In addition to mimicking reflective moving objects, the stirrer also provides a more controlled channel variation than the other types, which is crucial for fair comparison at different transmission frequencies and loading scenarios. It has been designed to resemble that used in a reverberation chamber [13]. It has a height of 410 mm, and sits on top of its motor, which has a height of 325 mm, and is located on the cavity floor, such that it obscures the direct line of sight between the antennas. The maximum radius of the stirrer is 230 mm, and it operates at 0.19 full rotations per second. Note that the stirrer was present in the cavity for all four tests, but was only switched on for the mechanical stirring measurement.

In the second measurement campaign (the results of which are presented in Section III-C), Schwarzbeck 9112 broadband antennas were used (to enable us to vary the operating frequency). The transmitting antenna was located at (180, 160, 830) mm and the receiving antenna at (980, 910, 510) mm, both x-polarized. The stirrer was used for every measurement, at the same rotational speed, and was again located between the antennas to obscure the direct line of sight. For the second measurement campaign, in order to draw conclusions regarding the variation of Doppler spread with frequency, we considered it more relevant to perform the measurements at regularly spaced frequencies over a large range, rather than to choose frequencies corresponding to specific wireless systems.

Fig. 4. (a) Car; (b) transmitting node located in the passenger side rear door; (c) receiving node located in the boot on the driver side.

Therefore, measurements were undertaken at 3, 6, 9, 12, and 15 GHz, with 0, 4, 8, and 12 units of Radar Absorbent Material (RAM). A single unit of RAM is shown in Fig. 3(b), and it consists of a square based pyramid with base of side 150 mm and vertical height 390 mm, on top of a cuboid of height 50 mm. Three single measurement sweeps were recorded for each RAM and frequency permutation.

C. Measurements in an Actual Road Vehicle

For comparison purposes, the initial measurement campaign detailed in Section II-B was repeated in the passenger compartment of a panel van, with the antennas located on the dashboard (transmitter), and by the driver side door (receiver). The van was stationary, with a person sitting in the driver's seat, pretending to drive (i.e., to represent the Doppler spread associated with driver motion). The presented measurement was the average over 50 single sweeps undertaken using the spectrum analyzer.

A second measurement campaign conducted in a road car was undertaken, where the temporal resolution was reduced, in return for tracking the variation of the channel throughout a whole journey (of duration 225 s). To achieve this, a wireless sensor network (WSN) system was deployed, based around *MICAz* [14] WSN nodes. The tests were undertaken in a road car, shown in Fig. 4, with one MICAz node acting as a transmitter and one MICAz node as a receiver. One node was set to constantly transmit at one packet each 0.125 s, at 2.45 GHz, while the other node received the packets and logged their Received Signal Strength Indicator (RSSI) values. The nodes have been calibrated, so that the RSSI values can be converted into received power (and hence signal magnitude). A third node was placed on the dashboard, and acted as a second receiver. The results from this second receiver were similar to those presented in this paper, and hence has not been included to avoid unnecessary repetition.

III. Rapid Channel Variation: Characterized as a Doppler Spread

A. Causes of Channel Variation With Time

There are four possible causes of the random channel variation with time. Before enumerating these causes we note that it has been shown that external objects have little influence on the propagation process in the vehicle cavity [3]. The primary causes of time variation are:

1) The random motion of absorptive objects in the cavity (absorptive stirring).
2) The random motion of reflective objects in the cavity (reflective stirring).
3) The random motion of one antenna (i.e., transmitter or receiver).
4) The random motion of both antennas (i.e., transmitter and receiver).

To understand the significance of these four channel time variation causes (i.e., 1–4 above), consider the propagation process in the vehicle cavity which has been shown to be analogous to that in the reverberation chamber [2], [3]. At sufficiently high frequencies (i.e., greater than 1.7 GHz [3]), the cavity exhibits a standing wave pattern. Variations caused by absorptive and reflective stirring can be considered to be a change in the boundary conditions of this standing wave pattern. Variations caused by the movement of one antenna can be considered to be a change in the initial condition of this standing wave pattern (i.e., by noting that the channel is reciprocal and choosing the moving antenna to be the transmitter). We would therefore expect to see a similar Doppler spread for variation causes 1–3. It also seems reasonable that the Doppler spread caused by both antennas moving should be similar to that of a single antenna moving, although possibly spread over a broader frequency. Our results are shown in Fig. 5. Note that for comparison we also show a measurement of the Doppler shift when a person sits in the road vehicle and pretends to drive (labeled 'Van').

As predicted, the Doppler spread is similar for variation causes 1–3. We note that for cause 4 (i.e., where both antennas are moved), we do not observe a broader Doppler spread, however it is not critical to this work to establish why this is the case. For the three stirring measurements (i.e., as opposed to moving antenna measurements), a non-negligible amount of the energy remains exactly at the carrier frequency (i.e., has a Doppler shift of 0 Hz). This is because the stirring does not in general disturb the whole field, an observation we revisit in Section IV. Heddebaut *et al.* have also addressed this issue by investigating the ratio of stirred energy to unstirred energy (which they define as the *stirring ratio*) for an in-vehicle channel, with measured values in the range 12–20 dB [15]. While to our knowledge there are no existing measurements of Doppler spreads in vehicles, there are results of Doppler spreads measured in reverberation chambers [7], [12], [16]–[19]. Of particular interest are the Doppler spreads presented in [12], where measurements were performed with the stirrer moving (i.e., equivalent to our variation cause 2), and also with a single antenna moving (i.e., equivalent to our variation cause 3). We note that the Doppler spread observed in the reverberation chamber (i.e., [[12] Figure 2]) has a similar shape to our measurements in the vehicle cavity (i.e., Fig. 5), as would be expected.

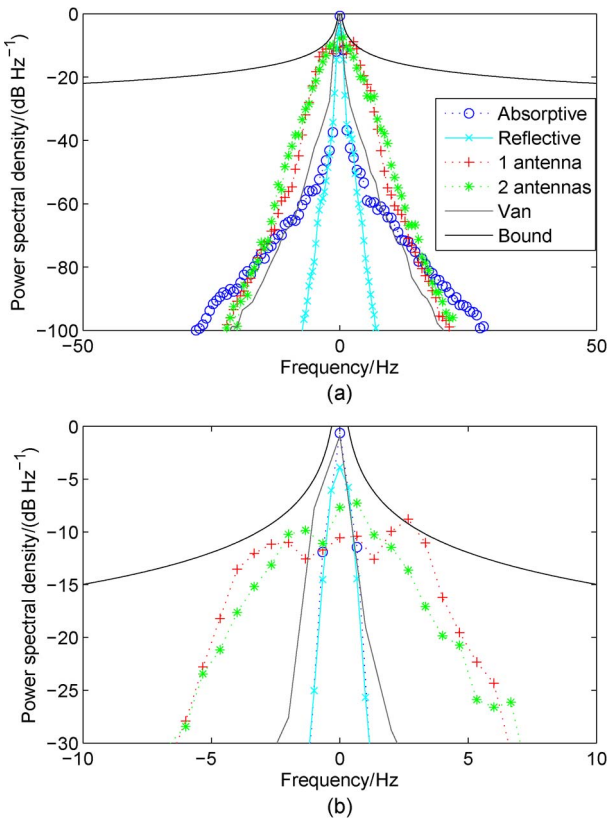

Fig. 5. Power spectral density at 2.45 GHz, for various channel variation causes: (a) Full range; (b) detailed close-up.

B. Doppler Spectrum Shape

The shape of the Doppler spectrum is by definition a function of the time variation of the channel, which in turn is a function of the random motion of the cavity occupants/antennas. It is beyond the scope of this work to model this as a statistical process, and indeed it would be hard to generalize such a model to all possible occupant movements. Moreover, as identified in the introduction, knowing the shape of the Doppler spectrum is not as important as knowing the maximum Doppler shift (i.e., so we can establish if $\tau_0\nu_0 \leq 1/4$). We can show some interesting properties of the PSD by making the following reasonable assumptions:

1) The channel is WSS- as already assumed when modeling the channel as WSSUS.
2) The autocorrelation function (ACF), $R_T(f, f; \zeta)$, at a time shift, ζ, is real and positive: this can be justified by considering that after the time shift, part of the signal will remain unaltered, and the rest we consider to be completely uncorrelated to the original signal. Note also, in general for a WSS process $R_T(f, f; \zeta) = R_T^*(f, f; -\zeta)$ (where * denotes complex conjugation), therefore as the autocorrelation function is real $R_T(f, f; \zeta) = R_T(f, f; -\zeta)$

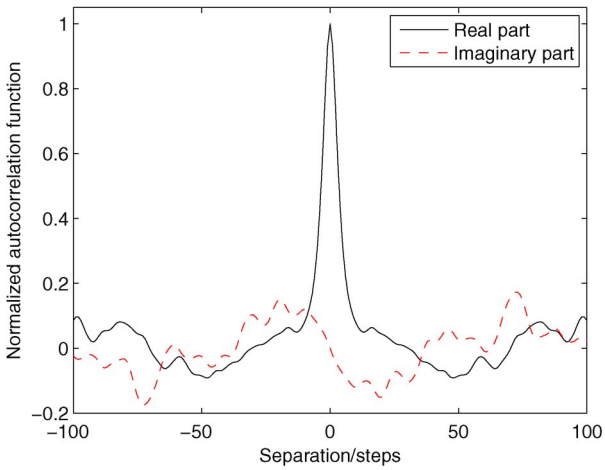

Fig. 6. Normalized autocorrelation function in the reverberation chamber, at 2 GHz.

3) $R_T(f, f; \zeta)$ decreases monotonically with increasing $|\zeta|$: i.e., the channel becomes less correlated with time.

We note that Assumption 2 is sufficient to ensure that the mean Doppler shift is zero. This is because the ACF is a real, even function, and thus its Fourier transform, the PSD, is also a real, even function. The mean Doppler shift is proportional to integral of the frequency variable, f, multiplied by the PSD [[20] Equation (3.28a)]. Since f is a real, odd function, and the PSD is a real, even function, the multiplication of the two is a real, odd function and thus the result is zero when it is integrated between the limits $-K$ and K. Letting K tend to infinity, we can see that the mean Doppler shift is equal to zero. For ACFs which have a continuous first derivative, this must be zero when the time separation is zero (i.e., in order for the function to be even), and this is consistent with the well-known property that the mean Doppler shift is proportional to the first derivative of the ACF, at zero time separation, if the first derivative exists [[20] Equation (3.29a)].

These assumptions are verified experimentally, as described in Section II-A. From Fig. 6 we can see that the ACF is indeed predominantly real, positive and monotonically decreasing with the magnitude of the number of paddle steps of separation.

We start from the definition of the PSD, $P_H(f, f; \nu)$ from [[5] Equation (6.28)]:

$$P_H(f,f;\nu) = \int_{-\infty}^{\infty} R_T(f,f;\zeta) e^{-j2\pi\nu\zeta} d\zeta,$$

$$= \int_{-\infty}^{\infty} R_T(f,f;\zeta)\cos(2\pi\nu\zeta) d\zeta, \quad (1)$$

$$< \int_{-\infty}^{\infty} R_T(f,f;\zeta) \times 1 \, d\zeta,$$

$$= P_H(f,f;0). \quad (2)$$

Therefore, the Doppler spread has a global maximum at the carrier frequency. Returning to (1), we can show a further interesting property of the PSD:

$$P_H(f,f;\nu) = \int_{-\infty}^{\infty} R_T(f,f;\zeta)\cos(2\pi\nu\zeta) d\zeta, \quad (3)$$

$$= 2\int_{0^+}^{\infty} R_T(f,f;\zeta)\cos(2\pi\nu\zeta) d\zeta, \quad (4)$$

$$= 2\left[\frac{1}{2\pi\nu}\sin(2\pi\nu\zeta) R_T(f,f;\zeta)\right]_{\zeta=0^+}^{\infty} + 2\int_{0^+}^{\infty} \frac{-dR_T(f,f;\zeta)}{d\zeta}\frac{\sin(2\pi\nu\zeta)}{2\pi\nu} d\zeta, \quad (5)$$

$$< \frac{1}{\pi\nu} R_T(f,f;\infty) + \frac{1}{\pi\nu}\left(R_T(f,f;0^+) - R_T(f,f;\infty)\right), \quad (6)$$

$$= \frac{1}{\pi\nu} R_T(f,f;0). \quad (7)$$

The term 0^+ denotes a point infinitesimally to the right of the origin, which given that the function is finite at all points leads to the same result as had the integration taken place from the origin itself. The term 0^+ is required, as it is necessary that the ACF is continuously differentiable throughout the region of the integration, and this is not necessarily the case at the origin, where a discontinuity in the gradient may occur. Note that in (7), 0^+ has been replaced with 0 as $R_T(f, f, \nu)$ is continuously varying with ν. Observe also that (5) leads to (6) since throughout the region of interest (i.e., $\zeta > 0$), $R_T(f, f; \zeta) > 0$ and $(-dR_T(f, f; \zeta)/d\zeta) > 0$, and using these properties $\sin(2\pi\nu\zeta)$ can be replaced with 1 to find an upper bound on both the integral and the term inside the square brackets. Also, note that we have abused nomenclature slightly, strictly speaking: $R_T(f, f; \infty) =_{K\to\infty} R_T(f, f; K)$.

We have therefore shown that the PSD has a global maximum at $\nu = 0$, and is bounded by a known monotonically decreasing function (i.e., $(1/\pi\nu)R_T(f, f; 0)$). These results provide some theoretical justification for assuming that our measured Doppler spreads are typical of those observed in vehicle cavities in general. It is also interesting to note that $R_T(f, f; 0)$ is the total received power (P_{rx}), which is necessarily smaller than or equal to the total transmitted power (P_{tx}), which allows us to state a further relationship:

$$P_H(f,f;\nu) < \frac{1}{\pi\nu} P_{rx}, \quad (8)$$

$$\leq \frac{1}{\pi\nu} P_{tx}. \quad (9)$$

This relationship provides a bound on the PSD which is potentially useful for system designers to establish at what Doppler frequency shift the received power becomes indistinguishable from the noise floor (i.e., to a given tolerance, for a known signal-to-noise-ratio). Fig. 5 shows the bound given in (8) alongside our Doppler spread measurements. It can be seen (i.e., in the zoomed in plot given in Fig. 5(b)) that the bound is

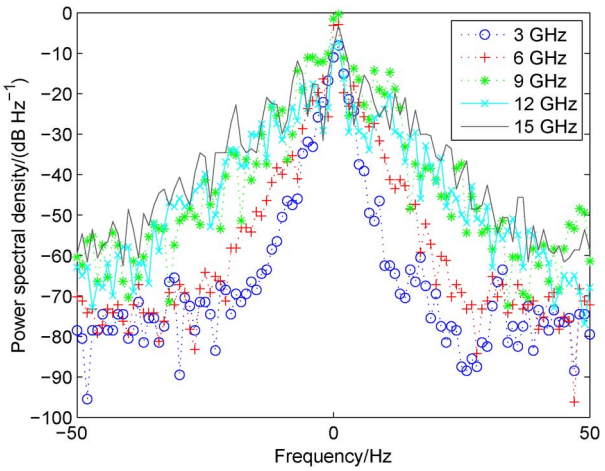

Fig. 7. Power spectral density at varying carrier frequencies (for the cavity not loaded with RAM).

violated only once, and only by a small amount. This violation occurs for the scenario where one antenna is moved, this is possibly as a result of the motion not being totally random, or perhaps owing to the fact that the input signal is not a perfect spike, as shown in Fig. 2.

The significance of this result is that while the PSD is theoretically supported over an infinite frequency range, in practice at some frequency shift, it will become indistinguishable from the noise-floor. In addition from (8) and (9) it can be shown that once this has happened, the power level will not re-emerge from below the noise floor (as would potentially be possible for Jakes' model [21]). Our measurements show $\nu_0 < 50$ Hz, τ_0 is of the order of 100 ns [2], [3], therefore $\tau_0\nu_0 \approx 5 \times 10^{-6} \leq 1/4$, which means we would expect to be able to approach the capacity of a channel with perfect receiver CSI.

It should be noted, that while for our purposes it is preferable merely to bound the PSD using a generally applicable set of assumptions, it is also possible to model the actual PSD itself by making a more rigid set of assumptions regarding the scatterer motion. Examples of such a model are derived by Pham *et al.* [22] and Borhani and Patzold [23].

C. Variation of Doppler Spread With Carrier Frequency and Cavity Loading

Having established the similarity between the Doppler spreads for the four types of variation in Section III-A, we now choose to focus solely on the time-variation arising due to the reflective stirrer to characterize the variation in Doppler spread with carrier frequency and cavity loading. This is because the mechanical stirrer rotates with constant angular velocity, ensuring a fair comparison for the different experimental arrangements (i.e., relying on human motion, while useful for obtaining the ground truth, is not particularly repeatable).

In the reverberation chamber, it has been shown theoretically (and verified experimentally) that the maximum Doppler shift is proportional to the carrier frequency [12], [16], [17]. As the propagation process in the vehicle cavity is analogous to that in the reverberation chamber, we expect the same relationship to hold in the vehicle cavity. Fig. 7 shows the Doppler shift in the cavity (not loaded with RAM) for a range of carrier frequencies. It is hard to precisely evaluate the maximum Doppler shift from a single measurement, however it is observed that the Doppler spread increases with increased carrier frequency.

Chen *et al.* [16] also address the variation of Doppler shift with cavity loading, in the reverberation chamber, finding that loading decreases the Doppler spread. We observe only a small decrease in Doppler spread with loading in the vehicle cavity, at all carrier frequencies, as shown in Fig. 8. A possible explanation for this is because in the reverberation chamber, the high Q factor environment is altered significantly by the introduction of the RAM, and hence the mode density (and therefore Doppler spread) also varies. In the vehicle cavity, it is likely that the presence of the four windows dominate the effect of the RAM, and hence there is no significant change in the mode density, and therefore the Doppler spread.

IV. Slow Channel Variation: Characterized in the Time Domain

As mentioned in the introduction, an important purpose for characterization of the slow channel variation is to improve communications performance through channel estimation. Specifically, we investigate whether we can predict the channel response. Measurements were undertaken in the time domain, as detailed in Section II-C, the raw data is shown in Fig. 9.

As previously noted in Section III-A, the received signal is the sum of an undisturbed field, and a stirred field. As shown in [3], at the frequency of operation the stirred field can be treated as isotropic, therefore we would expect the signal to be a random variable with a Rician probability density function. Fig. 10 provides some evidence that for our measurements, the Rician distribution is indeed appropriate (although the discretized form of the logged RSSI values somewhat limits the insight which can be gained from this plot).

Therefore, the simplest channel predictor, is one where each sample is simply treated as an independent identically distributed (i.i.d.) Rician random variable, and the Rician distribution parameters are estimated accordingly. Our stated aim is improved channel prediction compared to the simple Rician estimator where the predicted value is simply the mean of the maximum likelihood estimated Rician distribution from the samples up to that point.

A. Model for Time Correlation

Consider the time varying transfer function of the process, $T(f_0, t)$, (where $f_0 = 2.45$ GHz is the carrier frequency which is the same throughout) sampled at discrete time intervals (i.e., $T(f_0, t_n) = T(f_0, t_{n-1} + \tau)$). We continue to make assumptions 1–3 stated in Section III-B, and also make a further assumption:

4) $T(f_0, t_n)$ depends only on $T(f_0, t_{n-1})$, and not $T(f_0, t_{n-2}) \ldots T(f_0, t_0)$.

This assumption is made primarily for practical reasons, since it is unclear exactly how the correlation evolves in time,

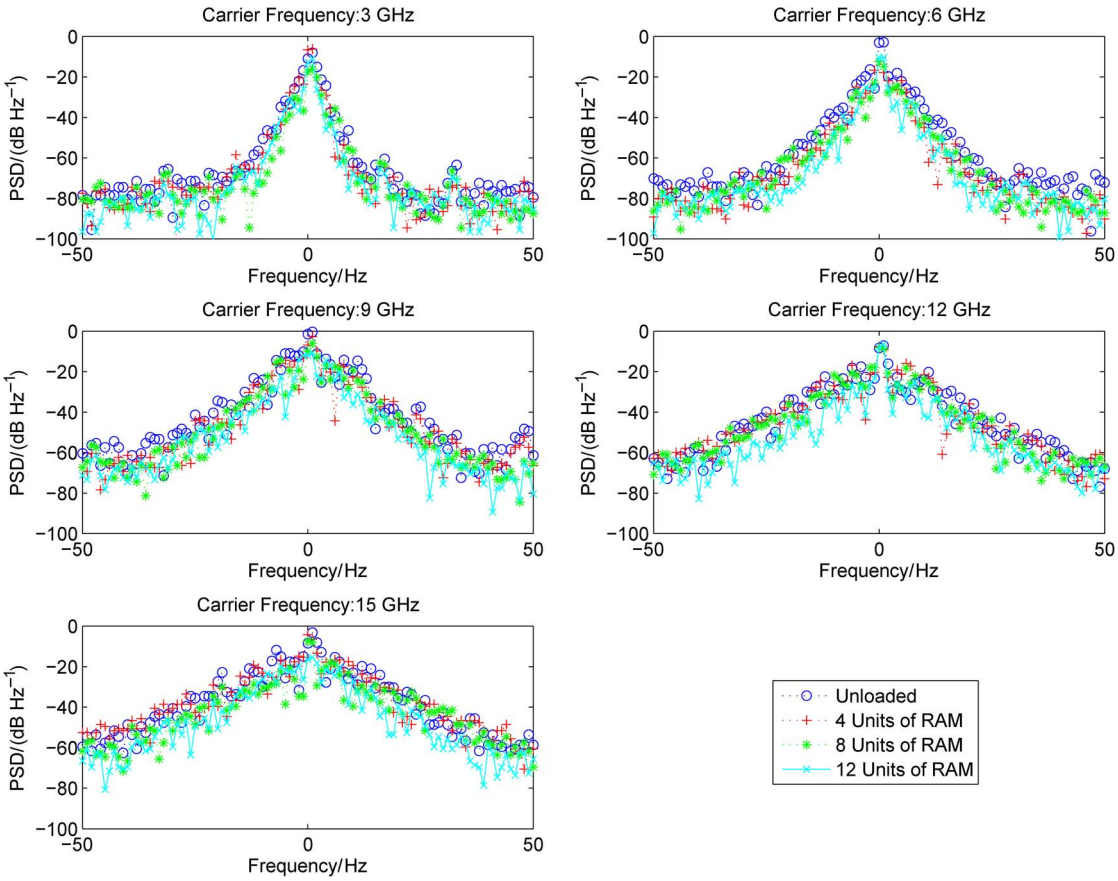

Fig. 8. Power spectral density with varying loading conditions and carrier frequencies.

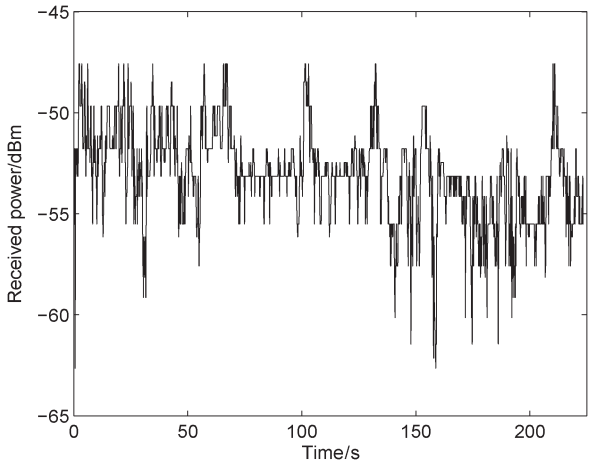

Fig. 9. Time series raw data, for a typical journey in the car with measurements performed using the MICAz based nodes.

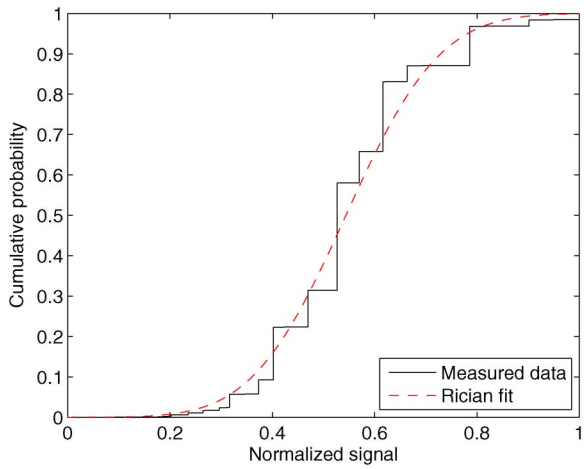

Fig. 10. Demonstration of Rician fit.

and thus making this simple assumption allows further analysis to be undertaken. The aim is to find an improved method of predicting the channel, rather than to uncover the actual underlying truth, and therefore the requirement on the validity of the assumptions made is significantly lower (i.e., if the resulting predictor leads to an improved estimate of the channel, then that alone is sufficient reason to make the assumption). There is however, some physical justification for making this assumption, which arises from the fact that occupant motion tends to be jerky and discontinuous, and furthermore the field which is being disturbed is itself chaotic, and therefore it is unlikely that the channel will evolve in a continuous way.

These assumptions (i.e., 1–4) are consistent with modeling the sampled time series as an AR1 process:

$$T(f_0, t_n) = A\,(T(f_0, t_{n-1}) - \mu) + \epsilon_n + \mu, \qquad (10)$$

where A is real, between zero and one, ϵ_n is an independent Gaussian random variable and μ is the process mean. Noting

that in general τ is arbitrary, we know that if the sampled process really is an AR1 process, then the underlying continuous time process must be an Ornstein-Uhlenbeck process [24], which has ACF:

$$\mathbb{E}\left(\left(T(f_0,t+\tau)-\mu\right)\left(T(f_0,t)-\mu\right)\right)=\sigma^2 e^{-\theta|\tau|}, \qquad (11)$$

where σ^2 is the process variance and θ is a constant and therefore, from (10), $A=e^{-\theta|\tau|}$. It should be noted that this is an example of an ACF which has a discontinuous first derivative at a time separation of zero, but still leads to a zero mean Doppler shift, because it is a real, even function.

Verifying for our measurements, that A does indeed approximately equal $e^{-\theta|\tau|}$ would provide some evidence that the assumptions are valid. It is, however, not possible to directly estimate the ACF (and therefore verify the exponential shape) from the measurements, as only the magnitude is available. Therefore, we take a slightly more sophisticated approach. Using (10) as a starting point:

$$\begin{aligned}&|T(f_0,t_n)|^2\\&\quad=\left|A\left(T(f_0,t_{n-1})-\mu\right)+\epsilon_n+\mu\right|^2, \qquad (12)\\&\quad=\left(A\,\mathrm{Re}\left(T(f_0,t_{n-1})\right)+(1-A)\mathrm{Re}(\mu)+\mathrm{Re}(\epsilon_n)\right)^2\\&\qquad+\left(A\,\mathrm{Im}\left(T(f_0,t_{n-1})\right)+(1-A)\mathrm{Im}(\mu)+\mathrm{Im}(\epsilon_n)\right)^2. \qquad (13)\end{aligned}$$

From (13), it can be shown:

$$\begin{aligned}\mathbb{E}\left(|T(f_0,t_n)|^2\,|T(f_0,t_{n-1})|^2\right)&=\alpha A^2+\beta A+\gamma, \qquad (14)\\&=\alpha e^{-2\theta|\tau|}+\beta e^{-\theta|\tau|}+\gamma, \qquad (15)\end{aligned}$$

where α, β, and γ are constants that depend on $\mathrm{Re}(\mu)$, $\mathrm{Im}(\mu)$, $\mathrm{Re}(\mu)\mathrm{Im}(\mu)$, $\mathbb{E}(\epsilon^2)$, $\mathbb{E}(\mathrm{Re}(\mu)^2)$, $\mathbb{E}(\mathrm{Im}(\mu)^2)$, $\mathbb{E}(\mathrm{Re}(\mu)\mathrm{Im}(\mu))$ and σ^2.

In addition, we use the measured data to apply the approximation $\mathbb{E}(|T(f_0,t_n)|^2|T(f_0,t_{n-1})|^2)\approx\langle|T(f_0,t_n)|^2|T(f_0,t_{n-1})|^2\rangle$ (where $\langle.\rangle$ is an average over the measured data), and find a minimum mean squared error (MMSE) fit for the parameters α, β, γ and θ. In Fig. 11 it can be seen that there is reasonable agreement between the theoretical and the measured power ACF values. The value of θ was found to be 0.475, which corresponds to a time constant of 2.11 s. The order of magnitude of this value is consistent with previous work investigating the stability of in-vehicle channels, where the coherence time was measured as 1–10 s [25], [26]. It should be noted, that while the observed fit is encouraging, the function has four degrees of freedom, and therefore this alone does not constitute unequivocal evidence that we have uncovered the underlying process.

B. Using an AR1 Process to Track the Time-Series

Having established that the Ornstein-Uhlenbeck model appears to be a good fit for the underlying process, but that the evidence from the ACF alone is not totally compelling, it is interesting to ask whether any real benefits can be achieved by modeling the time variation in this way. To do this, we consider a channel which transmits continuously at one packet every 0.125 s, on the same frequency channel (as detailed in Section II-C). We would like to use our proposed time variation model to predict the received power for the next packet, and as a reference we consider a simple predictor, where the signal magnitude is a Rician random variable, and each packet is treated as independent. As a starting point, we express (13) in a slightly different way:

$$|T(f_0,t_n)|^2=A^2\,|T(f_0,t_{n-1})|^2+(1-A)^2|\mu|^2+\epsilon_n', \qquad (16)$$

where ϵ' incorporates all of the other terms. In general, ϵ_n' is a random term, however it is not Gaussian, and not independent of $A^2|T(f_0,t_{n-1})|^2+(1-A)^2|\mu|^2$. However, if we treat ϵ_n' as a series of i.i.d. Gaussian random variables, we can see that (16) is in the form of an AR1 process, and we can investigate whether this leads to an improved prediction of the received power, compared to the simple i.i.d. Rician predictor. Fig. 12 shows that the AR1 process does indeed lead to an improved (i.e., reduced variance) prediction of the channel received power.

We observe that after approximately 75 s there appears to have been a step shift in received power. This is an example of the fact that the process is actually quasi-WSSUS [4] not WSSUS, and the channel estimation/prediction can be improved by introducing a forgetting factor or finite window length (i.e., to use as a sample to estimate the parameters). For our purposes, however, this is unnecessary, as we can see that the AR1 predictor consistently outperforms the Rician predictor both before and after 75 s.

In this section, we have shown that improved channel prediction can be achieved by modeling the time variation as an AR1 process. This has been derived theoretically from stated assumptions, and while not within the scope of this work, it would be interesting to investigate further the general validity of these assumptions. Also, a further refinement of the frequency domain characterization could be achieved if these assumptions

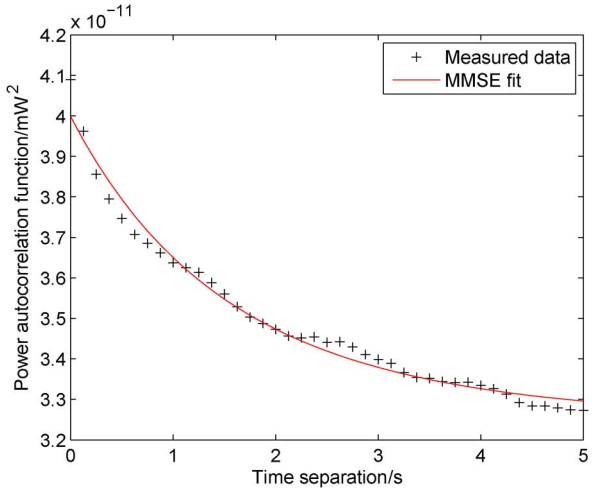

Fig. 11. Autocorrelation function of received power (not normalized).

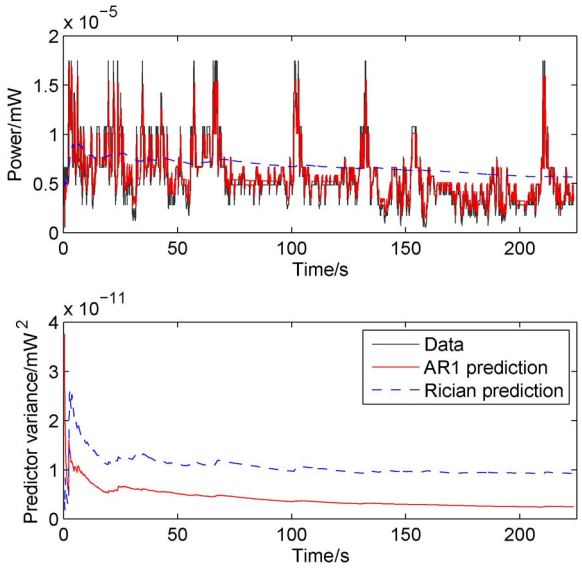

Fig. 12. Prediction of received power, comparing our proposed method to a simple Rician prediction.

are shown to be also valid for rapid time variation of the channel.

V. Conclusion

In this paper, we have sought to characterize the time variation of typical in-vehicle wireless communication channels to improve their performance. We have investigated the spectral properties of the in-vehicle channel by performing Doppler spread measurements in a metal cavity with vehicle like properties. Also, we have characterized the slow time variation of the in-vehicle channel by performing time domain measurements in an actual car.

We have identified four possible causes of channel time variation in the vehicle cavity: absorptive motion; reflective motion; one antenna moving; and both antennas moving. We have measured the Doppler shift for each case, observing that the Doppler spread shape is similar for each, and we have put forward some reasons why this is the case. Furthermore, we observe that the Doppler spread has a peak at the carrier frequency, decreasing as the Doppler frequency becomes further removed from the carrier frequency. Using physically reasonable assumptions, we have provided a theoretical justification for why this is the case. We note that this is an important property, as it means that the maximum Doppler shift is well-defined (to some tolerance), which in turn means that the coherence time is well defined, which is important for deploying effective communications systems. We find that the maximum Doppler shift is approximately 50 Hz, which means that the channel is underspread, and therefore it is possible to approach the capacity of a channel with perfect receiver CSI.

We measure the Doppler shift over a range of carrier frequencies, finding that the Doppler spread increases with carrier frequency, which is consistent with existing measurements in reverberation chambers. We also measure the Doppler spread at a range of cavity loading scenarios, finding no significant variation in Doppler spread. Previous studies have found that

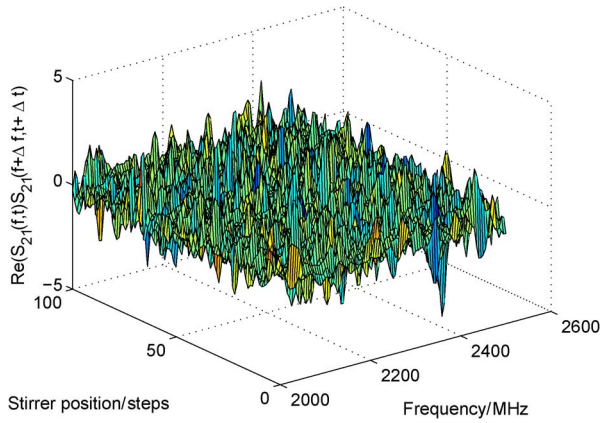

Fig. 13. Normalized $\mathrm{Re}(S_{21}(f,t) \times S_{21}(f+f', t+t'))$, for $f' = 5$ MHz and $t' = 1$ paddle step.

increased loading leads to reduced Doppler spreads in the reverberation chamber, however we reason that the presence of the windows in the vehicle cavity dominates any effect owing to the loading.

We also measure the time variation of the channel in an actual vehicle over a typical journey by recording the power received in transmitted packets every 0.125 s. We find that we can predict the received power using an AR1 process, with reduced variance compared to the case where we treat each value as an i.i.d. random variable.

Appendix A
Justification of the WSSUS Assumption

In the introduction, we reasoned that the time variation of the channel is likely to be well modeled as a WSSUS process. This means that at any time and frequency shift, the autocorrelation function of the channel is only a function of said time and frequency shift. It is difficult to show unequivocally that there is no dependence on other variables, however we can use the measurements detailed in Section II-A to provide some evidence that there appears to be no dependence on absolute time or frequency.

Fig. 13 shows a surface of the real part of $S_{21}(f,t) \times S_{21}(f+\Delta f, t+\Delta t)$, for $\Delta f = 5$ MHz and $\Delta t = 1$ paddle step (i.e., there are 1000 paddle steps in a whole rotation, and therefore if the angular velocity is known, it is possible to express Δt in terms of time). We observe that there appears to be no dependence on the absolute value of time and frequency. We plotted the surface for various values of Δt and Δf with similar results.

This evidence, together with the theoretical reasoning, leads us to proceed to further analyze the time variation of the in-vehicle channel, assuming that it can be modeled as a WSSUS process.

Acknowledgment

The authors would like to thank David Knight for his help with the Doppler spread measurements.

REFERENCES

[1] J. Dawson, D. Hope, M. Panitz, and C. Christopoulos, "Wireless networks in vehicles," in *Proc. IET Semin. Electromagn. Propag. Struct. Buildings*, Dec. 2008, pp. 1–6.

[2] S. Herbert, T. H. Loh, and I. Wassell, "An impulse response model and Q-factor estimation for vehicle cavities," *IEEE Trans. Veh. Technol.*, vol. 62, no. 9, pp. 4240–4250, Nov. 2013.

[3] S. J. Herbert, I. Wassell, T.-H. Loh, and J. Rigelsford, "On the analogy between vehicle cavities and reverberation chambers," *IEEE Trans. Antennas Propag.* [Online]. Available: http://www.cl.cam.ac.uk/~sjh227/vehrev.pdf

[4] P. Bello, "Characterization of randomly time-variant linear channels," *IEEE Trans. Commun. Syst.*, vol. CS-11, no. 4, pp. 360–393, Dec. 1963.

[5] J. D. Parsons, *The Mobile Radio Propagation Channel*, 2nd ed. Hoboken, NJ, USA: Wiley, 2000.

[6] A. Goldsmith, *Wireless Communications*. Cambridge, U.K.: Cambridge Univ. Press, 2005.

[7] X. Chen, "Evaluation and measurement of the Doppler spectrum in a reverberation chamber," *Progr. Electromagn. Res. M*, vol. 26, pp. 267–277, 2012.

[8] G. Durisi, U. Schuster, H. Bolcskei, and S. Shamai, "Noncoherent capacity of underspread fading channels," *IEEE Trans. Inf. Theory*, vol. 56, no. 1, pp. 367–395, Jan. 2010.

[9] C. E. Shannon, "A mathematical theory of communication," *Bell Syst. Tech. J.*, vol. 27, no. 3, pp. 379–423, Jul.–Oct. 1948. [Online]. Available: http://cm.bell-labs.com/cm/ms/what/shannonday/shannon1948.pdf

[10] G. Durisi, H. Bolcskei, and S. Shamai, "Capacity of underspread WSSUS fading channels in the wideband regime," in *Proc. IEEE Int. Symp. Inf. Theory*, 2006, pp. 1500–1504.

[11] H. Zhang, J. Rigelsford, L. Low, and R. Langley, "Field distributions within a rectangular cavity with vehicle-like features," in *Proc. LAPC*, Loughborough, U.K., Mar. 2008, pp. 205–208.

[12] K. Karlsson, X. Chen, P.-S. Kildal, and J. Carlsson, "Doppler spread in reverberation chamber predicted from measurements during step-wise stationary stirring," *IEEE Antennas Wireless Propag. Lett.*, vol. 9, pp. 497–500, May 2010.

[13] J. F. Dawson and L. Arnaut, Reverberation (Mode-Stirred) Chambers for Electromagnetic Compatibility. [Online]. Available: http://www.compliance-club.com/archive/old_archive/030530.htm

[14] [Online]. Available: http://www.memsic.com/wireless-sensor-networks/

[15] M. Heddebaut, V. Deniau, and K. Adouane, "In-vehicle WLAN radio-frequency communication characterization," *IEEE Trans. Intell. Transp. Syst.*, vol. 5, no. 2, pp. 114–121, Jun. 2004.

[16] X. Chen, P.-S. Kildal, and J. Carlsson, "Determination of maximum Doppler shift in reverberation chamber using level crossing rate," in *Proc. 5th EUCAP*, 2011, pp. 62–65.

[17] P. Hallbjorner and A. Rydberg, "Maximum Doppler frequency in reverberation chamber with continuously moving stirrer," in *Proc. LAPC*, Loughborough, U.K., 2007, pp. 229–232.

[18] S. M. H. A. Shah, "Wireless channel characterization of the reverberation chamber at NIST," M.S. thesis, Dept. Signals Syst., Chalmers Univ. Technol., Gothenburg, Sweden, 2011.

[19] P. Corona, G. Ferrara, and M. Migliaccio, "A spectral approach for the determination of the reverberating chamber quality factor," *IEEE Trans. Electromagn. Compat.*, vol. 40, no. 2, pp. 145–153, May 1998.

[20] M. Patzold, *Mobile Radio Channels*, 2nd ed. Hoboken, NJ, USA: Wiley, 2012.

[21] W. C. Jakes, *Microwave Mobile Communications*. New York, NY, USA: Wiley-Interscience, 1974.

[22] V.-H. Pham, M. H. Taieb, J.-V. Chouinard, S. Roy, and H.-T. Huynh, "On the double Doppler effect generated by scatterer motion," *REV J. Electromagn. Commun.*, vol. 1, no. 1, pp. 30–37, Mar. 2011.

[23] A. Borhani and M. Patzold, "Correlation and spectral properties of vehicle-to-vehicle channels in the presence of moving scatterers," *IEEE Trans. Veh. Technol.*, vol. 62, no. 9, pp. 4228–4239, Nov. 2013.

[24] M. Sørensen, Ornstein–Uhlenbeck Process, Hoboken, NJ, USA: Wiley, 2006. [Online]. Available: http://dx.doi.org/10.1002/9780470012505.tao009m

[25] H.-M. Tsai *et al.*, "Feasibility of in-car wireless sensor networks: A statistical evaluation," in *Proc. 4th Annu. IEEE Commun. Soc. Conf. SECON Mesh Ad Hoc*, 2007, pp. 101–111.

[26] A. Moghimi, H.-M. Tsai, C. Saraydar, and O. Tonguz, "Characterizing intra-car wireless channels," *IEEE Trans. Veh. Technol.*, vol. 58, no. 9, pp. 5299–5305, Nov. 2009.

Steven Herbert (S'12) received the B.A. degree [subsequently promoted to M.A. (Cantab) in 2013] and the M.Eng. degree from the University of Cambridge, Cambridge, U.K., in 2010, where he is currently working toward the Ph.D. degree.

He is currently with the Digital Technologies Group, Computer Laboratory, University of Cambridge, and the Electromagnetic Technologies Group, National Physical Laboratory, Teddington, U.K.

Ian Wassell received the B.Sc. and B.Eng. degrees from Loughborough University, Loughborough, U.K., in 1983 and the Ph.D. degree from the University of Southampton, Southampton, U.K., in 1990. He is currently a Senior Lecturer with the Computer Laboratory, University of Cambridge, Cambridge, U.K., and has more than 15 years of experience in the simulation and design of radio communication systems gained via a number of positions in industry and higher education. He has published more than 190 papers concerning wireless communication systems, and his current research interests include fixed wireless access, sensor networks, cooperative networks, propagation modeling, compressive sensing, and cognitive radio. He is a Chartered Engineer and a member of the IET.

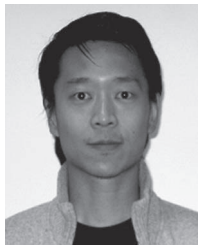

Tian-Hong Loh (S'03–M'05) was born in Johor, Malaysia. He received the B.Eng. degree (first class) from Nottingham Trent University, Nottingham, U.K., in 1999 and the Ph.D. degree from the University of Warwick, Coventry, U.K., in 2005, both in electrical and electronic engineering. In 2005, he joined the National Physical Laboratory, Teddington, U.K., as a Higher Research Scientist, and since 2009, he has been a Senior Research Scientist, involved in work on fundamental research and develop measurement technologies in support of the electronics and communication industry. Since 2011, he has been appointed as RF and Microwave Technical Theme Leader, involved in physical program formulation and strategy development. His current research interests include metamaterials, computational electromagnetics, small antenna, smart antennas, multiple-input–multiple-output antennas, and wireless sensor networks.

Jonathan Rigelsford (SM'13) received the M.Eng. and Ph.D. degrees in electronic engineering from the University of Hull, Hull, U.K., in 1997 and 2001, respectively. From 2000 to 2002, he was a Senior Design Engineer with Jaybeam Ltd., designing antennas for cellular base stations. From late 2002 until 2014, he was a Senior Experimental Officer for the Communications Group with the Department of Electronic and Electrical Engineering, University of Sheffield, Sheffield, U.K., where he is currently a Senior Research Fellow. His current research interests include RF propagation, adaptive antennas, RFID, and cyber security. Dr. Rigelsford was an Active Member of the Antenna Interface Standards Group from 2002 to 2010 being elected to the board of directors during that time. More recently, he has become the Secretary to the Wireless Friendly Building Forum, an industrial/academic initiative to promote understanding of radio propagation within the built environments.